1 **Impact of NOₓ and OH on secondary organic aerosol (SOA) formation**
2 **from β-pinene photooxidation**

3 **Mehrnaz Sarrafzadeh[1,3], Jürgen Wildt[2], Iida Pullinen[1], Monika Springer[1], Einhard Kleist[2],**
4 **Ralf Tillmann[1], Sebastian H. Schmitt[1], Cheng Wu[1], Thomas F. Mentel[1], Donald R. Hastie[3],**
5 **and Astrid Kiendler-Scharr[1]**

7 1. Institute for Energy and Climate Research, IEK-8, Forschungszentrum Jülich, 52425, Jülich,
8 Germany

9 2. Institute of Bio- and Geosciences, IBG-2, Forschungszentrum Jülich, 52425, Jülich,
10 Germany

11 3. Centre for Atmospheric Chemistry, York University, 4700 Keele St., Toronto, ON M3J 1P3,
12 Canada

14 Correspondence to: J. Wildt (j.wildt@fz-juelich.de)

1 **Abstract**

2 In this study, the NO_x dependence of secondary organic aerosol (SOA) formation from β-pinene

3 photooxidation was comprehensively investigated in the Jülich Plant Atmosphere Chamber.

4 Consistent with the results of previous NO_x studies we found increases of SOA yields at low

5 NO_x conditions ($[NO_x]_0 < 30$ ppb, $[BVOC]_0/[NO_x]_0 > 10$ ppbC ppb^{-1}). Furthermore, increasing

6 $[NO_x]$ at high NO_x conditions ($[NO_x]_0 > 30$ ppb, $[BVOC]_0/[NO_x]_0$ ~10 to ~2.6 ppbC ppb^{-1})

7 suppressed the SOA yield. The increase of SOA yield at low NO_x conditions was attributed to

8 increase of OH concentration, most probably by OH recycling in $NO + HO_2 \rightarrow NO_2 + OH$

9 reaction. Separate measurements without NO_x addition but with different OH primary production

10 rates confirmed the OH dependence of SOA yields. After removing the effect of OH

11 concentration on SOA mass growth by keeping the OH concentration constant, SOA yields only

12 decreased with increasing $[NO_x]$. Measuring the NO_x dependence of SOA yields at lower

13 $[NO]/[NO_2]$ ratio showed less pronounced increase in both; OH concentration and SOA yield.

14 This result was consistent to our assumption of OH recycling by NO and to SOA yields being

15 dependent on OH concentrations. It furthermore indicated that NO_x dependencies vary for

16 different NO_x compositions. A substantial fraction of the NO_x-induced decrease of SOA yields at

17 high NO_x conditions was caused by NO_x-induced suppression of new particle formation (NPF).

18 This was shown by probing the NO_x dependence of SOA formation in the presence of seed

19 particles. After eliminating the effect of NO_x-induced suppression of NPF and NO_x induced

20 changes of OH concentrations, the overall effect of NO_x on the SOA yield from β-pinene

21 photooxidation was moderate. Comparing with β-pinene experiments, the SOA formation from

22 α-pinene photooxidation was only suppressed by increasing NO_x. However, basic mechanisms of

23 the NO_x impacts were the same as that of β-pinene.

1. Introduction

Biogenic volatile organic compounds (BVOC), such as monoterpenes ($C_{10}H_{16}$) are emitted in large quantities into the atmosphere (Guenther et al., 1995, 2012; Griffin et al., 1999a). These BVOCs are oxidized in the atmosphere by hydroxyl radicals (OH), ozone (O_3), or nitrate radicals (NO_3) resulting in the formation of secondary organic aerosol (SOA). SOA contributes to a substantial fraction of ambient organic aerosol and is known to adversely affect visibility, climate and human health (Hallquist et al., 2009).

SOA formation potentials of BVOC species are represented by SOA yields which are generally defined as the ratio of the SOA mass produced from the oxidation of the SOA precursor to the mass of the precursor consumed (Odum et al., 1996). Despite the fact that many studies have focused on the production of SOA from a number of monoterpenes, reported SOA yields have shown high variability for a given precursor (Pandis et al., 1991; Hoffmann et al., 1997; Griffin et al., 1999b; Larsen et al., 2001; Presto et al., 2005; Kroll et al., 2006; Ng et al., 2007; Mentel et al., 2009; Eddingsaas et al., 2012a). For instance, the reported SOA mass yield for α-pinene photooxidation ranges from 8 % to 37 % (Eddingsaas et al., 2012a). This variability is likely related to the numerous factors that influence the SOA yields, such as the inorganic and organic mass loading, particle acidity, NO_x ($NO_x = NO + NO_2$) level, humidity, and temperature. Therefore, ambient SOA yields cannot be represented by a unique value for a given monoterpene as the yields are heavily dependent on the conditions under which the SOA is formed.

One of the critical factors is the impact of NO_x on SOA formation. Results of the majority of studies indicate that SOA yields are lower at high NO_x levels (Hatakeyama et al., 1991; Pandis et al., 1991; Presto et al., 2005; Kroll et al., 2006; Ng et al., 2007). It is generally assumed that the impact of NO_x results from altering the balance between competing peroxy-radical (RO_2)

1   reactions and thus from the changes in the distribution of oxidation products. Reaction (R1) is

2   the dominant pathway for RO_2 radicals under low-NO_x conditions which leads to the formation

3   of low-volatility hydroperoxides that can participate in new particle formation (NPF) and

4   contribute to SOA mass (Johnson et al., 2005; Camredon et al., 2007).

5    $RO_2 + HO_2 \rightarrow ROOH + O_2$ (R1)
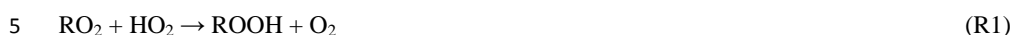
6   Under high-NO_x conditions, RO_2 radicals react with NO resulting in the formation of organic

7   nitrates (R2a) which are suggested to be relatively volatile as well as alkoxy radicals (R2b) that

8   either fragment, or react to form more volatile products. This understanding implies that higher

9   NO_x concentrations will suppress the formation of low volatility products, and thereby suppress

10   NPF and SOA mass formation.

11   $NO + RO_2 \rightarrow RONO_2$ (R2a)

12   $NO + RO_2 \rightarrow RO + NO_2$ (R2b)

13   Despite numerous studies of SOA formation from terpene ozonolysis, the SOA formation from

14   OH oxidation of β-pinene has been scarcely investigated. In the present study we investigated the

15   SOA formation from β-pinene photooxidation under varied NO_x levels in the Jülich Plant

16   Atmosphere Chamber (JPAC) to gain more insight into the impact of NO_x on SOA yield. Since

17   the [BVOC]/[NO_x] ratio varies significantly in urban atmospheres, the quantification of the

18   effect of NO_x on SOA yield of biogenic precursors is needed to better predict air pollution and to

19   improve the accuracy of current ambient models.

1 **2. Experimental**

2 The experimental setup of JPAC is described in detail elsewhere (Mentel et al., 2009, 2015). The

3 chamber is 1450 litre in volume, made of borosilicate glass and set up in a climate-controlled

4 housing. Temperature and relative humidity inside the chamber were held constant at $16 \pm 1^{o}C$

5 and $63 \pm 2\%$, respectively over the course of the experiments. The chamber was operated as a

6 continuously stirred tank reactor with a residence time of approximately 46 min. The flow into

7 the chamber consisted of two purified air streams. One stream was passed through an ozonator

8 and was humidified with double distilled water. The other stream contained β-pinene emitted

9 from a diffusion/permeation source held at 38°C. Where necessary seed particles could be

10 generated externally and introduced using a third air stream.

11 The chamber was equipped with several lamps; 12 discharge lamps (HQI 400 W/D; Osram) to

12 simulate the solar light spectrum in the chamber, 12 discharge lamps (Phillips, TL 60 W/10-R,

13 60W, λmax =365 nm, from here on termed UVA lamps) for NO_2 photolysis, and one internal

14 UVC lamp (Philips, TUV 40W, λmax =254 nm; here termed as TUV lamp) for ozone photolysis

15 to produce OH radicals by reaction of water vapour with $O(^1D)$ atoms. The TUV lamp could be

16 shielded by glass tubes to control the amount of UV radiation entering the chamber. Thus, by

17 altering the gap between these glass tubes, the OH production rate could be adjusted by varying

18 the photolysis rate $J(O^1D)$. It has to be noted that the short wavelength cut off of the glass is

19 around 350 nm and thus no light with wavelength short enough to produce O^1D is in the chamber

20 when the TUV lamp is off. Furthermore, the absorption cross section of NO_2 at the wavelength

21 of the TUV lamp is more than an order of magnitude lower than at wavelengths around 365 nm

22 (Davidson et al., 1988). Together with the quite low energy of the TUV lamp compared to the

23 energy of the UVA lamps, this allowed varying $J(O^1D)$ and $J(NO_2)$ independent of each other.

1   A suite of instruments were used to measure both the gas and particle phase products. Ozone

2   concentration was determined by UV photometric devices (Thermo Environmental 49 and

3   Ansyco, O_3 42M ozone analyzers), NO was measured by chemiluminescence (Eco Physics, CLD

4   770 AL ppt), NO_2 by chemiluminescence after photolysis (Eco Physics, PLC 760) and relative

5   humidity was measured by dew point mirror (TS-2, Walz). Furthermore, a condensation particle

6   counter (CPC, TSI 3783) and a scanning mobility particle sizer (SMPS, combination of a TSI

7   3081 electrostatic classifier and a TSI 3025 CPC) were used to count the total particle number

8   greater than 3 nm and to measure the particle size distribution between 13 and 740 nm

9   respectively. The total particle mass concentration was estimated from the measured total aerosol

10   volume assuming a SOA density of ~ 1.2 g cm^{-3} and spherical particles. β-pinene mixing ratio in

11   the chamber was determined by gas chromatography–mass spectrometry (GC-MS, Agilent GC-

12   MSD system with HP6890 GC and 5973 MSD) and a proton transfer reaction mass spectrometer

13   (PTR-MS, Ionicon). The GC-MS and PTR-MS were switched periodically between the outlet

14   and the inlet of the chamber to quantify concentrations of β-pinene entering and exiting the

15   chamber. The OH concentration was estimated from the decay of β-pinene in the chamber (Eq.

16   2) (Kiendler-Scharr et al., 2009).

$$\frac{d[\beta p]}{dt} = \frac{F}{V} \cdot ([\beta p]_{in} - [\beta p]) - (k^{OH} \cdot [OH] + k^{O3} \cdot [O_3]) \cdot [\beta p] \tag{1}$$

$$[OH] = \frac{\frac{F}{V} \cdot \frac{[\beta p]_{in} - [\beta p]}{[\beta p]} - k^{O3} \cdot [O_3]}{k^{OH}} \tag{2}$$

17   Equation (1) is the basic rate equation for a continuously stirred tank reactor resulting from mass

18   balance and Eq. (2) results from Eq. (1) under steady state conditions when solving for [OH]. In

19   Eqs. (1) and (2), V is the volume of the chamber and F is the total air flow through the chamber.

1   $[\beta p]_{in}$ and $[\beta p]$ are the concentrations of β-pinene in the inlet air and in the chamber, respectively.

2   For a well-mixed continuously stirred tank reactor, $[\beta p]$ is the concentration of β-pinene

3   measured in the outlet flow. k^{OH} and k^{O3} are the rate constants of reactions of β-pinene with OH

4   and with O_3. Since β-pinene has a quite low rate constant with O_3 (k^{O3} =1.5 × 10^{-17} cm^3 s^{-1}

5   (Atkinson and Arey, 2003)), the reaction of β-pinene with O_3 could be neglected from Eq. (2) for

6   our ozone- (50-100 ppb) and OH concentrations ($9 \times 10^{6} - 1.6 \times 10^{8}$ cm^{-3}). The uncertainty in

7   OH concentration was estimated to be approximately 20% (Wildt et al., 2014).

8   SOA yields were determined as described in Mentel et al. (2009), by calculating incremental

9   yields from the formed particle mass as a function of consumed precursor mass. However,

10   different from the procedure described in Mentel et al. (2009), here we use particle masses

11   corrected for wall losses of extremely low volatile organic compounds (ELVOC) that are direct

12   particle precursors.

13   Briefly, wall losses and losses on particles were determined for the ELVOCs. Using the

14   respective loss rates, the fraction of ELVOCs contributing to particle mass formation (dependent

15   on particle surface) and the fraction of ELVOCs lost on chamber walls were calculated. The ratio

16   of total loss rate divided by loss on particles was taken as correction factor allowing the

17   determination of the particle mass that would have been obtained if there were no wall losses.

18   Experiments with α-pinene and β-pinene verified the correction procedure for a wide range of

19   particle surfaces. The derivation of the correction method is described in detail in the

20   supplement. Note that this procedure is only valid for the chamber used in these experiments.

21   Additionally, we used another approach to determine the mass yields at steady state conditions.

22   Correcting measured particle masses by the above mentioned procedure revealed that after an

1   induction time of ~ 20 minutes, the wall loss corrected particle mass was constant as long as the

2   OH production rate was constant. This allowed determining yields using steady state

3   assumptions. Yields were determined by dividing the particle mass formed in the experiment by

4   the oxidation rate of the BVOC. At our method of [OH] determination, using the BVOC

5   consumption according to Eq. (2), and at the negligible inflow of particle mass into the chamber,

6   this equals the simple mass balance assumption: produced particle mass divided by BVOC

7   consumption (Eq. 3).

$$Y = \frac{Particle\ mass}{BVOC\ consumption} \tag{3}$$

8   As was expected from the consistency of wall loss corrected particle masses, both procedure of

9   yield determinations led to identical results. However, the method using steady state conditions

10   had advantages since adjustments of [OH] were required during many experiments. The

11   justification to use both type of yield determinations is given in the supplement.

2.1. Experimental procedure

13   A series of β-pinene photooxidation experiments were performed in the JPAC to investigate the

14   SOA formation under low-NO$_x$ (here defined as: [NO$_x$]$_0$ < 30 ppb, [BVOC]$_0$/[NO$_x$]$_0$ > 10) and

15   high-NO$_x$ (here defined as: [NO$_x$]$_0$ > 30 ppb, [BVOC]$_0$/[NO$_x$]$_0$< 10) conditions. In these

16   experiments, the inflow of β-pinene (95 %, Aldrich) to the chamber was kept constant, leading to

17   initial mixing ratios of 37 ± 0.6 ppb. Initial O$_3$ concentration was 40 ± 5 ppb. NO$_2$ (Linde, 104 ±

18   3 ppm NO$_2$ in nitrogen) was introduced into the β-pinene air stream. Initial NO$_x$ concentrations,

19   [NO$_x$]$_0$, in the chamber were varied between < 1 ppb and 146 ppb. The chamber was illuminated

20   with one of the HQI lamps and all the UVA lamps, resulting in an NO$_2$ photolysis frequency

21   (J(NO$_2$)) of 4.3×10^{-3} s^{-1}. When VOC-, NO$_x$- and O$_3$ concentrations in the chamber were near to

1   steady state, the experiment was initiated by turning on the TUV lamp resulting in OH radical

2   production. During the described experiments, a constant $J(O^1D)$ was maintained. Experiments

3   without NO_x addition were performed between NO_x experiments. In these cases, residual NO_x

4   concentrations from chamber walls were below 1 ppb.

5   After initiating the OH production, β-pinene and NO_x concentrations decreased due to their

6   reactions with OH radicals. The majority of the results presented in this study are from steady

7   state measurements, when all physical and chemical parameters were constant in the chamber.

8   However, for the purpose of comparison with the literature data, the initial concentration of NO_x,

9    $[NO_x]_0$, and β-pinene, $[BVOC]_0$, were also used here.

10   To investigate the role of NO_x on SOA formation in the presence of inorganic aerosol, β-pinene

11   photooxidation/NO_x experiments were repeated in the presence of seed aerosol. Seed particles

12   were generated from a 40 mg/L aqueous $(NH_4)_2SO_4$ solution, passed through a diffusion drier

13   and then introduced into the chamber. For these experiments, the organic particle mass was

14   determined by subtracting the initial seed aerosol mass from the total particle mass.

15   **3.   Results and discussion**

16   **3.1. Impact of NO_x on SOA formation**

17   To determine the influence of NO_x on SOA formation, a series of NO_x experiments were

18   conducted in the JPAC in which β-pinene was oxidized in the absence of inorganic seed aerosol.

19   A summary of experimental conditions and results for the β-pinene/NO_x photooxidation

20   experiments is given in Table 1. Figure 1 shows SOA yields, calculated from wall-loss corrected

21   maximum particle mass concentration (PM_{max}), as a function of $[BVOC]_0/[NO_x]_0$ ratio and

22   $[NO_x]_0$. The strong dependence of SOA yield on BVOC/NO_x levels is evident. At low NO_x

1   conditions an increase in the initial NO_x concentration increases the SOA yield, whereas at high

2   NO_x concentrations the opposite SOA yield dependence on NO_x was observed. Similar NO_x

3   dependencies of SOA yields have been observed in previous studies (Pandis et al., 1991; Kroll et

4   al., 2006; Zhang et al., 1992; Camredon et al., 2007).

5   At high NO_x conditions strong depletion of SOA yield as well as NPF was observed with

6   increasing NO_x (Fig. 1). Wildt et al. (2014) made similar observations for NPF during the

7   photooxidation of a BVOC mix emitted from Mediterranean plants. However, the NO_x

8   dependence of SOA yield was differed from that shown by Wildt et al. (2014). At low NO_x

9   concentrations we observed an increasing SOA yield with increasing NO_x (Fig. 1). At high NO_x

10   levels, the yields decreased. Having different NO_x dependencies at different NO_x regimes

11   suggests multiple factors at play.

12   Kroll et al. (2006) suggested that the increase in SOA yield with NO_x could be due to changes in

13   the $[NO]/[HO_2]$ ratio. As experiments in batch reactors proceed, NO_x concentrations decrease

14   due to their reactions with OH resulting in a switch from high NO_x to low NO_x conditions. The

15   lowered NO concentrations cause increasing HO_2 concentrations due to reaction (R3):

16     $NO + HO_2 \rightarrow NO_2 + OH$ (R3)

17   In such experiments, peroxy radicals initially react mainly with NO, whereas peroxy radicals

18   formed later from first generation products, primarily react with HO_2. Although the reason for

19   the observed increase of SOA yield with increasing NO_x at low NO_x levels was not fully

20   explored, Camredon et al. (2007) noted that this could be due to the influence of OH levels.

21   However, in the majority of studies investigating the impact of NO_x on SOA formation, OH

1 concentration was either not measured or the potential influence of OH was not discussed

2 (Eddingsaas et al., 2012a, 2012b).

3 As the NO_x concentration is changed in this study, the concentration of OH was found to change

4 markedly (Fig. 2). OH concentrations passed through a maximum (~ 3.8 x 10^7 molecules cm^{-3}) at

5 $[NO_x]_{ss}$ ~40 ppb ($[NO_x]_0$ ~ 70 ppb) which represented a fourfold increase over that in the absence

6 of NO_x. NO_x enhanced OH production in two ways: by increasing $[O_3]$ and thereby the

7 photolytic OH source, and by recycling OH through reaction (R3). However, at very high NO_x

8 concentrations, NO_x is acting as a sink for OH due to Reaction (R4):

9 $NO_2 + OH (+M) \rightarrow HNO_3 (+M)$ (R4)

10 Therefore, as illustrated in Fig. 2, OH concentration increased rapidly with increasing NO_x,

11 reached a maximum value and then decreased gradually. In general terms this is consistent with

12 the nonlinear dependence of OH concentration on NO_x level in the lower Troposphere (Ehhalt

13 and Rohrer, 1995).

14 It appeared in Fig. 2 that the SOA yields were somehow related to [OH]. Thus, we performed

15 some experiments to further explore the dependence of SOA formation on OH concentration.

3.1.1. [OH] dependence of SOA mass formation

17 To examine whether or not SOA yield depends on the OH concentration, additional experiments

18 were performed at two different OH production rates and the β-pinene concentration varied to

19 give a range of SOA mass. The detailed experimental conditions are summarized in Table 2.

20 Two different $J(O^1D)$ conditions ($1.9 \pm 0.2 \times 10^{-3}$ s^{-1} and $5.4 \pm 0.5 \times 10^{-3}$ s^{-1}) were used to give

21 significantly different OH production rates at otherwise unchanged conditions. Figure 3 shows

1   particle mass as a function of consumed β-pinene ranging from 20 to 140 µg m^{-3}. Approximately

2   90-95 % of the total β-pinene was consumed in these experiments.

3   The OH concentrations were $4 \times 10^7 - 1 \times 10^8$ molecules cm^{-3} and $1.1 - 1.6 \times 10^8$ molecules

4   cm^{-3} under low and high OH conditions, respectively. The SOA yields (incremental yields, see

5   Mentel et al., (2009) and the supplement to this paper) were higher at higher OH levels (31 ± 3

6   % and 20 ± 1 % for high and low OH conditions, respectively).

7   In discussing possible reasons for the OH impact, it is crucial to consider secondary reactions. As

8   an example, the rate constant for the reaction of β-pinene + OH is higher than that of the reaction

9   of nopinone + OH. Nopinone is a major product of β-pinene oxidation (Atkinson and Arey,

10   2003). Thus in the stirred flow reactor, where the oxidation of β-pinene does not go to

11   completion, there is an appreciable concentration of nopinone. Increasing the OH concentration

12   will therefore result in more nopinone consumption and, if nopinone oxidation also forms SOA

13   mass, this additional oxidation forms more SOA mass. As a result, SOA mass will be higher at

14   higher OH concentrations and thus, SOA yield based on the consumption of β-pinene will be

15   higher. Similarly, such sequential OH reactions can also form SOA mass in reactions with other

16   β-pinene oxidation products. Another possibility might be the OH dependence of ELVOCs

17   formation. Formation of such molecules might require more than one OH reaction.

18   From our data we cannot decide which process plays a major role for the OH dependence of

19   yields. Nevertheless, the results of these experiments affirm the importance of actual OH

20   concentrations in SOA mass formation. This complicates the assignment of the observed changes

21   in SOA yield to the impact of NO$_x$ on peroxy radical chemistry, as SOA yield was also likely

1   varied with [OH]. Thus, we undertook a series of experiments to decouple the impacts of OH and

2   NO_x on SOA formation.

3   **3.1.2. Isolate the effect of [OH] on SOA formation**

4   To examine the impact of NO_x on SOA production independent of [OH]-changes, a series of

5   experiments were performed where the steady state OH concentration was held constant by

6   tuning the value of $J(O^1D)$. This required constant [OH] monitoring as the system approached

7   steady state, i.e. monitoring the consumption of β-pinene, to ensure the [OH] was adjusted to the

8   desired level. Although there was a significant variation in initial OH concentrations on adding

9   NO_x if $J(O^1D)$ was unchanged, it was possible to maintain the OH concentrations to within 5 %

10   across all NO_x concentrations by adjusting $J(O^1D)$ (Fig. 4). Figure 5 shows the SOA yield as a

11   function of $[NO_x]$ during the steady state before and after [OH] adjustment. Before adjusting

12   [OH] the yield profile was consistent with our previous results; SOA yield increased with

13   increasing NO_x at low NO_x levels and then dropped at high NO_x levels. After adjusting [OH], the

14   yield revealed no increase at low NO_x levels. It was only suppressed by increasing NO_x. This

15   indicated that the observed increase in SOA yield without adjusting [OH] is a result of NO_x

16   enhancing [OH] and not a direct impact of NO_x on the SOA production. Thus isolating the effect

17   of [OH] revealed that increasing $[NO_x]$ only suppressed particle mass formation, and therefore

18   also suppressed SOA mass yield.

19   **3.2. Role of NO/NO_2 ratio in SOA formation**

20   We also investigated the effect of the $[NO]/[NO_2]$ ratio on SOA formation from β-pinene/NO_x

21   mixtures. To change this ratio we changed $[O_3]$. Ozone, NO and NO_2 are interrelated as

22   illustrated in Reactions (R5) and (R6):

1    $NO + O_3 \rightarrow NO_2 + O_2$ (R5)

2    $NO_2 + O_2 + h\upsilon \rightarrow NO + O_3$ (R6)

3   Neglecting reactions of NO with peroxy radicals the [NO]/[NO$_2$] ratio can then be described by

4   the photostationary steady state (Leighton, 1961):

$$\frac{[NO]}{[NO_2]} = \frac{J(NO_2)}{k^5[O_3]}$$ (4)

5   where $J(NO_2)$ represents the photolysis rate of Reaction (R6) and k^5 is the rate coefficient of

6   Reaction (R5). Hence, adjusting [O$_3$] in the chamber allowed varying [NO]/[NO$_2$] ratios. Here,

7   to probe the dependency of SOA mass formation on relative NO and NO$_2$ concentrations, NO$_x$

8   experiments were performed with approximately 50 % higher O$_3$ concentration (74 ± 7 ppb) than

9   that of previous NO$_x$ experiments. The remaining conditions maintained the same.

10   Results obtained from these experiments are shown in Fig. 6. The behaviour observed in the

11   high-O$_3$ experiments (equivalent to lower NO/NO$_2$) was different from that in the experiments

12   with the lower [O$_3$]. When not adjusted, [OH] increased with increasing NO$_x$ but the increase

13   was less pronounced. With a lower [NO]/[NO$_2$] ratio, the maximum OH concentration increase

14   was approximately twofold relative to the respective NO$_x$ free experiments (Fig. 6), compared to

15   the fourfold increase with the higher [NO]/[NO$_2$] (Fig. 4). This is consistent to the assumption

16   that reaction (R3) recycles OH. There was also a slight increase in SOA yield when [NO$_x$]

17   increased up to ~15 ppb. In addition, the increase in SOA yield was less pronounced in the high-

18   O$_3$ experiments again pointing to the role of [OH] in SOA formation.

19   The role of [OH] was also confirmed by another observation. By comparing the data without

20   NO$_x$ addition, it can be seen that [OH] as well as the yields are higher in the high-O$_3$

1 experiments. The higher $[O_3]$ caused a higher OH production rate and at otherwise same

2 conditions ($J(O^1D)$, $[H_2O]$, etc.), higher [OH] and thereby higher yields. In summary, the results

3 of the high-O_3 experiments confirmed our interpretations of the results from the low-O_3

4 experiments and again supported the key role of actual OH concentrations in SOA mass

5 formation.

6 After adjusting [OH] to the same level as in the NO_x free experiments (Fig. 6), no increase in

7 SOA yield was observed and increasing NO_x only suppressed SOA formation (Fig. 7). These

8 results were consistent with those found earlier in the low-O_3 experiments indicating that, after

9 isolating the effect of [OH], SOA yield was only suppressed with increasing NO_x also at higher

10 $[O_3]$. Comparing the yield profiles obtained from the low-O_3 and the high-O_3 experiments

11 respectively (blue circles in Fig. 5 and Fig. 7), it can be seen that the decrease in SOA yield was~

12 35 % in the high-O_3 experiments while it was roughly 70 % in the low-O_3 experiments. This

13 shows that NO_x dependencies itself depend on the composition of NO_x. As the suppression of

14 yield was more pronounced in the low-O_3 experiments (= higher $[NO]/[NO_2]$) it seemed that NO

15 is the molecule mainly responsible for the SOA yield diminishing effect of NO_x.

16 **3.3. Comparison of the impact of NO_x on SOA yield from α-pinene and β-pinene**

17   **photooxidation**

18 A series of α-pinene/NO_x experiments were performed in the same chamber to compare the NO_x

19 dependencies of SOA formation of α-pinene to that of β-pinene. These experiments were

20 performed with 12 ± 1.2 ppb α-pinene, 78 ± 14 ppb O_3 and with $[NO_x]_0$ up to 126 ppb.

21 When using α-pinene as the SOA precursor, no increase in aerosol mass formation was observed

22 at low NO_x, with only suppression of the particle mass formation and the SOA yield (Fig. 8).

1   Furthermore, presumably due to the lower α-pinene concentrations, no particle formation at all

2   was observed when $[NO_x]_0$ was above 60 ppb.

3   At high NO_x levels, the differences between the NO_x dependencies of α-pinene (Fig. 8) and β-

4   pinene (Fig. 1) photooxidation were not very strong, both showing a decrease with increasing

5   NO_x. At low NO_x levels there were substantial differences, in that β-pinene showed a distinctive

6   increase and maximum of the yield, while the yield of α-pinene is almost unaffected and

7   monotonically decreasing. These differences can be explained by the differences in $[O_3]$ during

8   α-pinene and β-pinene photooxidation. The lower $[O_3]$ in the β-pinene experiments caused

9   higher $[NO]/[NO_2]$ ratios and thus more effective conversion of HO_2 to OH by NO (reaction R3).

10   This is supported by the experiments with β-pinene performed at higher $[O_3]$ that caused less

11   NO_x induced increase of [OH] (Fig. 6, black squares), as well as less NO_x induced increase of

12   SOA yield (Fig. 7, black circles). Restricting focus to the same $[BVOC]/[NO_x]$ where the

13   substantial increase in β-pinene SOA yield was observed (> 100 to ~20 ppbC ppb^{-1}), such

14   increases were neither observed for α-pinene nor for the monoterpene mix emitted from

15   Mediterranean species (Wildt et al., 2014). The NO_x dependence of SOA formation therefore is

16   different in different chemical systems. As the SOA yield was dependent on the actual OH

17   concentrations, differences in OH recycling may be involved here as well. However at high NO_x

18   conditions, the principle behaviour of all systems was identical; a general SOA yield suppression

19   with increasing NO_x.

20   **3.4. Impact of NO_x on SOA formation in the presence of seed aerosol**

21   From Fig. 2, it can be seen that the SOA yield measured at $[NO_x]_{ss}$ ~ 86 ppb ($[NO_x]_0$ ~ 146 ppb)

22   was lower than that at $[NO_x]_0$ < 1 ppb while [OH] was higher. Hence, there must be another

23   effect of NO_x addition besides its impact on [OH]. As illustrated in Fig. 9, particle number

1   concentrations were suppressed significantly when adding NO_x. The strong decrease of particle

2   number concentration with increasing NO_x indicates that NPF is suppressed by NO_x (see also

3   Wildt et al., 2014). Hence, there is a high chance that the SOA formation is hindered by low

4   particle phase condensational sinks at high NO_x levels and thus, the observed suppression of

5   SOA yield may be due to the suppression of NPF. At high NO_x conditions, particle numbers and

6   surfaces were quite low. Therefore, high correction factors had to be used to correct the particle

7   mass for wall losses of ELVOCs which includes high uncertainties (see supplement). These

8   uncertainties can be diminished by using seed particles since they provide a surface onto which

9   the low volatile organics may condense. In the presence of seed aerosol, the growth of particles

10   would not be limited by the surface of particles and would be much less affected by losses of

11   SOA-precursors on the chamber walls.

12   Therefore, experiments with variations of $[NO_x]$ were also conducted in the presence of

13   ammonium sulfate $((NH_4)_2SO_4)$ seed particles (average seed mass and surface were

14   approximately 9 ± 1 µg m^{-3} and 1.3×10^{-3} m^2 m^{-3}, respectively). These experiments were carried

15   out in the same manner as previous experiments; by adjusting [OH] during steady state to the

16   same level as during the NO_x free experiments. Figure 10 presents a comparison of SOA yield

17   before and after [OH] adjustment for seeded NO_x experiments (seed mass is subtracted from the

18   total particle mass to determine the organic mass used in the yield calculation). The results from

19   the seeded experiments showed the same general features as the unseeded experiments. Without

20   adjustment of [OH], yields increased with increasing NO_x at low levels and were slightly

21   suppressed with further increasing NO_x. The most evident difference here to the experiments

22   without seed is the fairly high yield at high $[NO_x]$ (Fig. 10). Even after [OH] was adjusted, the

23   decrease in SOA yield was not as significant as in the experiments without seed particles. This

1   suggests that in the absence of seed particles, the accumulation of mass was indeed limited by

2   low particle surface caused by the NO_x induced suppression of NPF.

3   In the presence of seed particles and at constant [OH], the decrease in yield was only moderate.

4   This indicates that other NO_x impacts such as formation of organic nitrates were moderate as

5   well. The difference between yields determined with and without addition of seed particles

6   indicates that at very small particle surface, our correction procedure underestimates wall losses

7   of precursors. This might be due to either possible differences in uptake of the ELVOC by

8   particles (mainly organic particles versus ammonium sulfate particles), or the differences in the

9   size of particles. However, the real reason for this underestimation is not known yet.

10   Our correction procedure may involve uncertainties and errors. Nevertheless, it had to be

11   applied; otherwise the NO_x dependence would have been overestimated. NO_x suppresses NPF

12   and thereby limits mass formation in the absence of seed particles. As both, the impacts of wall

13   losses and impacts of suppressed NPF on SOA mass formation are certainly diminished in the

14   presence of seed, we assume that the experiments with seed particles give the most reliable

15   results on direct NO_x impacts on SOA mass formation from β-pinene.

16   **4. Summary and Conclusions**

17   We investigated the effect of NO_x on SOA formation from β-pinene photooxidation under low

18   NO_x and high NO_x conditions and found a very similar behaviour as that observed in other

19   studies (Pandis et al., 1991; Zhang et al., 1992; Presto et al., 2005; Kroll et al., 2006; Camredon

20   et al., 2007; Pathak et al., 2007; Chan et al., 2010; Hoyle et al., 2011; Loza et al., 2014). At low

21   NO_x levels SOA yields increased with increasing NO_x and then decreased at higher NO_x

22   concentrations. The increase of yield at low $[NO_x]$ was caused by the NO_x induced increase of

1   [OH]. The decrease of yield at higher NO_x levels was mainly a consequence of NPF suppression

2   and thereby decreasing particle condensational sink with increasing NO_x. Eliminating the

3   impacts of NO_x on NPF and on [OH], showed that the impacts of NO_x on mass formation were

4   only moderate. Even at the highest NO_x level ($[NO_x]_{ss} \sim 86$ ppb, $[BVOC]_{ss}/[NO_x]_{ss} \sim 1.1$)

5   suppression of mass yield was only $20 - 30$ %. VOC/NO_x ratios in typical urban air are often

6   much higher than the $[BVOC]/[NO_x]$ range scanned here (Cai et al., 2011; Pollack et al., 2013;

7   Zou et al., 2015). Therefore dependent on the conditions, impacts of NO_x on SOA formation in

8   the real atmosphere may be far less than 20-30 %.

9   Our study also showed that SOA yield is dependent on OH concentration. Although the exact

10   mechanism for this [OH] dependence is still unknown, our results show that besides yield

11   dependencies on the amount of pre-existing matter and effects like partitioning there is also a

12   dependence on reaction conditions, in particular on oxidant levels. Although SOA yields

13   measured in laboratory chambers may not be indicative of the yields in the real atmosphere, their

14   variations as a consequence of different conditions could provide a more comprehensive

15   description of SOA in global and climate model.

16   **Acknowledgements**

17   This work was supported by the European Commission's 7th Framework Program under Grant

18   Agreement Number 287382 (Marie Curie Training Network PIMMS).

1 **References**

2 Atkinson, R., and Arey, J.: Atmospheric degradation of volatile organic compounds, Chem.

3 Rev., 103, 4605-4638, doi:10.1021/cr0206420, 2003.

4 Cai, C., Kelly, J. T., Avise, J. C., Kaduwela, A. P. and Stockwell, W. R.: Photochemical

5 modeling in California with two chemical mechanisms: model intercomparison and response to

6 emission reductions, J. Air Waste Manage. Assoc., 61(5), 559–572, doi:10.3155/1047-

7 3289.61.5.559, 2011.

8 Camredon, M., Aumont, B., Lee-Taylor, J. and Madronich, S.: The SOA/VOC/NO_x system: an

9 explicit model of secondary organic aerosol formation, Atmos. Chem. Phys., 7(21), 5599–5610,

10 doi:10.5194/acp-7-5599-2007, 2007.

11 Chan, A. W. H., Chan, M. N., Surratt, J. D., Chhabra, P. S., Loza, C. L., Crounse, J. D., Yee, L.

12 D., Flagan, R. C., Wennberg, P. O. and Seinfeld, J. H.: Role of aldehyde chemistry and NO_x

13 concentrations in secondary organic aerosol formation, Atmos. Chem. Phys., 10(15), 7169–7188,

14 doi:10.5194/acp-10-7169-2010, 2010.

15 Davidson, J. A., Cantrell, C. A., McDaniel, A. H., Shetter, R. E., Madronich, S. and Calvert, J.

16 G.: Visible-ultraviolet absorption cross sections for NO_2 as a function of temperature, J.

17 Geophys. Res. Atmos., 93(D6), 7105–7112, doi:10.1029/JD093iD06p07105, 1988.

18 Eddingsaas, N. C., Loza, C. L., Yee, L. D., Chan, M., Schilling, K. A., Chhabra, P. S., Seinfeld,

19 J. H. and Wennberg, P. O.: alpha-pinene photooxidation under controlled chemical conditions -

20 Part 2: SOA yield and composition in low- and high-NO_x environments, Atmos. Chem. Phys.,

21 12(16), 7413–7427, doi:10.5194/acp-12-7413-2012, 2012a.

22 Eddingsaas, N. C., Loza, C. L., Yee, L. D., Seinfeld, J. H. and Wennberg, P. O.: α-pinene

23 photooxidation under controlled chemical conditions – Part 1: Gas-phase composition in low-

24 and high-NO_x environments, Atmos. Chem. Phys., 12(14), 6489–6504, doi:10.5194/acp-12-

25 6489-2012, 2012b.

26 Ehhalt D.H., and Rohrer F.: The impact of commercial aircraft on tropospheric ozone, In: "The

27 Chemistry of the Atmosphere - Oxidants and Oxidation in the Earth's Atmosphere", A.R. Bandy

28 (Ed.), The Royal Society of Chemistry, Special Publication No. 170, p. 105-120, 1995.

29 Griffin, R. J., Cocker, D. R., Seinfeld, J. H. and Dabdub, D.: Estimate of global atmospheric

organic aerosol from oxidation of biogenic hydrocarbons, Geophys. Res. Lett., 26(17), 2721–2724, doi:10.1029/1999GL900476, 1999a.

Griffin, R. J., Cocker, D. R., Flagan, R. C. and Seinfeld, J. H.: Organic aerosol formation from the oxidation of biogenic hydrocarbons, J. Geophys. Res., 104(D3), 3555–3567, doi:10.1029/1998JD100049, 1999b.

Guenther, A., Hewitt, C. N., Erickson, D., Fall, R., Geron, C., Graedel, T., Harley, P., Klinger, L., Lerdau, M., Mckay, W. A., Pierce, T., Scholes, B., Steinbrecher, R., Tallamraju, R., Taylor, J. and Zimmerman, P.: A global model of natural volatile organic compound emissions, J. Geophys. Res., 100(D5), 8873, doi:10.1029/94JD02950, 1995.

Guenther, A. B., Jiang, X., Heald, C. L., Sakulyanontvittaya, T., Duhl, T., Emmons, L. K. and Wang, X.: The model of emissions of gases and aerosols from nature version 2.1 (MEGAN2.1): an extended and updated framework for modeling biogenic emissions, Geosci. Model Dev., 5(6), 1471–1492, doi:10.5194/gmd-5-1471-2012, 2012.

Hallquist, M., Wenger, J. C., Baltensperger, U., Rudich, Y., Simpson, D., Claeys, M., Dommen, J., Donahue, N. M., George, C., Goldstein, A. H., Hamilton, J. F., Herrmann, H., Hoffmann, T., Iinuma, Y., Jang, M., Jenkin, M. E., Jimenez, J. L., Kiendler-Scharr, A., Maenhaut, W., McFiggans, G., Mentel, T. F., Monod, A., Prévôt, A. S. H., Seinfeld, J. H., Surratt, J. D., Szmigielski, R. and Wildt, J.: The formation, properties and impact of secondary organic aerosol: current and emerging issues, Atmos. Chem. Phys., 9(14), 5155–5236, doi:10.5194/acp-9-5155-5236, 2009.

Hatakeyama, S., Izumi, K., Fukuyama, T., Akimoto, H. and Washida, N.: Reactions of OH with α-pinene and β-pinene in air: Estimate of global CO production from the atmospheric oxidation of terpenes, J. Geophys. Res., 96(D1), 947–958, doi:10.1029/90JD02341, 1991,

Hoffmann, T., Klockow, D., Odum, J., Bowman, F., Collins, D., Flagan, R. C. and Seinfeld, J. H.: Formation of Organic Aerosols from the Oxidation of Biogenic Hydrocarbons, J. Atmos. Chem., 26(2), 189–222, doi:10.1023/A:1005734301837, 1997.

Hoyle, C. R., Boy, M., Donahue, N. M., Fry, J. L., Glasius, M., Guenther, A., Hallar, A. G., Huff Hartz, K., Petters, M. D., Petäjä, T., Rosenoern, T. and Sullivan, A. P.: A review of the anthropogenic influence on biogenic secondary organic aerosol, Atmos. Chem. Phys., 11(1),

321–343, doi:10.5194/acp-11-321-2011, 2011.

Johnson, D., Jenkin, M. E., Wirtz, K. and Martin-Reviejo, M.: Simulating the Formation of Secondary Organic Aerosol from the Photooxidation of Aromatic Hydrocarbons., Sect. Title Air Pollut. Ind. Hyg., 2(1), 35–48, doi:10.1071/EN04079, 2005.

Kiendler-Scharr, A., Wildt, J., Dal Maso, M., Hohaus, T., Kleist, E., Mentel, T. F., Tillmann, R., Uerlings, R., Schurr, U. and Wahner, A.: New particle formation in forests inhibited by isoprene emissions, Nature, 461(7262), 381–384, doi:10.1038/nature08292, 2009.

Kroll, J. H., Ng, N. L., Murphy, S. M., Flagan, R. C. and Seinfeld, J. H.: Secondary organic aerosol formation from Isoprene photooxidation, Environ. Sci. Technol., 40(6), 1869–1877, doi:10.1021/es0524301, 2006.

Larsen, B. R., Di Bella, D., Glasius, M., Winterhalter, R., Jensen, N. R. and Hjorth, J.: Gas-phase OH oxidation of monoterpenes: Gaseous and particulate products, J. Atmos. Chem., 38(3), 231–276, doi:10.1023/A:1006487530903, 2001.

Leighton, P. A.: photochemistry of Air pollution., 1961.

Loza, C. L., Craven, J. S., Yee, L. D., Coggon, M. M., Schwantes, R. H., Shiraiwa, M., Zhang, X., Schilling, K. A., Ng, N. L., Canagaratna, M. R., Ziemann, P. J., Flagan, R. C. and Seinfeld, J. H.: Secondary organic aerosol yields of 12-carbon alkanes, Atmos. Chem. Phys., 14(3), 1423–1439, doi:10.5194/acp-14-1423-2014, 2014.

Mentel, Th. F., Wildt, J., Kiendler-Scharr, A., Kleist, E., Tillmann, R., Dal Maso, M., Fisseha, R., Hohaus, Th., Spahn, H., Uerlings, R., Wegener, R., Griffiths, P. T., Dinar, E., Rudich, Y., and Wahner, A.: Photochemical production of aerosols from real plant emissions, Atmos. Chem. Phys., 9(13), 4387–4406, doi:10.5194/acp-9-4387-2009, 2009.

Mentel, T. F., Springer, M., Ehn, M., Kleist, E., Pullinen, I., Kurtén, T., Rissanen, M., Wahner, A. and Wildt, J.: Formation of highly oxidized multifunctional compounds: autoxidation of peroxy radicals formed in the ozonolysis of alkenes – deduced from structure–product relationships, Atmos. Chem. Phys., 15(12), 6745–6765, doi:10.5194/acp-15-6745-2015, 2015.

Ng, N. L., Chhabra, P. S., Chan, A. W. H., Surratt, J. D., Kroll, J. H., Kwan, A. J., McCabe, D. C., Wennberg, P. O., Sorooshian, A., Murphy, S. M., Dalleska, N. F., Flagan, R. C., and

1   Seinfeld, J. H.: Effect of NOx level on secondary organic aerosol (SOA) formation from the
2   photooxidation of terpenes, Atmos. Chem. Phys., 7(4), 5159–5174, doi:10.5194/acp-7-5159-
3   2007, 2007.

4   Odum, J. R., Hoffmann, T., Bowman, F., Collins, D., Flagan, R. C. and Seinfeld, J. H.:
5   Gas/Particle partitioning and secondary organic aerosol yields, Environ. Sci. Technol., 30(8),
6   2580–2585, doi:10.1021/es950943+, 1996.

7   Pandis, S. N., Paulson, S. E., Seinfeld, J. H. and Flagan, R. C.: Aerosol formation in the
8   photooxidation of isoprene and β-pinene, Atmos. Environ. Part A, Gen. Top., 25(5-6), 997–1008,
9   doi:10.1016/0960-1686(91)90141-S, 1991.

10 Pathak, R. K., Presto, A. A., Lane, T. E., Stanier, C. O., Donahue, N. M. and Pandis, S. N.:
11 Ozonolysis of α-pinene: parameterization of secondary organic aerosol mass fraction, Atmos.
12 Chem. Phys., 7(14), 3811–3821, doi:10.5194/acp-7-3811-2007, 2007.

13 Pollack, I. B., Ryerson, T. B., Trainer, M., Neuman, J. A., Roberts, J. M. and Parrish, D. D.:
14 Trends in ozone, its precursors, and related secondary oxidation products in Los Angeles,
15 California: A synthesis of measurements from 1960 to 2010, J. Geophys. Res. Atmos., 118(11),
16 5893–5911, doi:10.1002/jgrd.50472, 2013.

17 Presto, A. A., Huff Hartz, K. E. and Donahue, N. M.: Secondary organic aerosol production from
18 terpene ozonolysis. 2. eEffect of NO_x concentration, Environ. Sci. Technol., 39(18), 7046–7054,
19 doi:10.1021/es050400s, 2005.

20 Wildt, J., Mentel, T. F., Kiendler-Scharr, A., Hoffmann, T., Andres, S., Ehn, M., Kleist, E.,
21 Muesgen, P., Rohrer, F., Rudich, Y., Springer, M., Tillmann, R. and Wahner, A.: Suppression of
22 new particle formation from monoterpene oxidation by NO_x, Atmos. Chem. Phys., 14(6), 2789–
23 2804, doi:10.5194/acp-14-2789-2014, 2014.

24 Zhang, S.-H., Shaw, M., Seinfeld, J. H. and Flagan, R. C.: Photochemical aerosol formation from
25 α-pinene- and β-pinene, J. Geophys. Res., 97(D18), 20717, doi:10.1029/92JD02156, 1992.

26 Zou, Y., Deng, X. J., Zhu, D., Gong, D. C., Wang, H., Li, F., Tan, H. B., Deng, T., Mai, B. R.,
27 Liu, X. T. and Wang, B. G.: Characteristics of 1 year of observational data of VOCs, NO_x and O_3
28 at a suburban site in Guangzhou, China, Atmos. Chem. Phys., 15(12), 6625–6636,
29 doi:10.5194/acp-15-6625-2015, 2015.

Table 1. Experimental conditions and results for β-pinene/NOx photooxidation experiments.

β-pinene reacted (ppb)	[NOx]0 (ppb)[a]	[NOx]ss (ppb)[b]	[OH]/10^7 (cm^-3)	PMmax (μg m^-3)[c]	PMss (μg m^-3)[d]	J3 (cm^-3 s^-1)[e]	[BVOC]0/[NOx]0 (ppbC ppb^-1)	SOA yield[f] (%)	SOA yield[g] (%)
33.9	73.9	34.4	3.7	30.3	----	0.9	5.2	15.7	----
34.0	54.8	35.5	3.7	37.6	34.4	7.8	7.0	19.3	17.7
30.4	145.9	86.1	1.8	14.3	----	0.04	2.6	8.2	----
31.4	13.4	9.5	2.2	33.1	31.7	48.9	28.6	18.4	17.7
33.1	102.5	45.7	3.0	27.2	27.2	0.4	3.7	14.4	14.5
33.5	32.9	21.7	3.3	38.2	40.2	25.5	11.7	20.0	21.0
29.4	6.7	5.1	1.5	30.9	30.3	50.3	57.0	18.4	18.0
23.7	<0.5	<1.0	0.8	20.0	17.7	41.3	765	14.7	13.1
25.3	<0.5	<1.0	0.9	23.5	22.1	57.5	768	16.2	15.3
25.7	<0.5	<1.0	0.9	24.4	22.8	62.0	768	16.6	15.5
25.3	<0.5	<1.0	0.9	23.8	22.5	54.2	768	16.5	15.6
25.7	<0.5	<1.0	1.0	22.9	22.8	53.8	767	15.6	15.5

[a] Initial NOx concentration before OH production
[b] NOx concentration during steady state, in cases without NOx addition we found increasing NOx which is assumed to be produced from residual HNO3 that is photolyzed by the TUV lamp.
[c] Maximum formed particle mass concentration, assuming an SOA density of 1.2 g cm^-3. These values have been adjusted for wall losses and losses on particles.
[d] Particle mass concentration during steady state, assuming an SOA density of 1.2 g cm^-3. These values have been adjusted for wall losses and losses on particles.
[e] Rates of new particle formation for particles greater than 3 nm
[f] SOA yields determined from PMmax
[g] SOA yields determined from PMss

1 **Table 2.** Experimental conditions and results for β-pinene photooxdation experiments at two OH
2 levels.

$J(O^1D)/10^{-3}$ (s^{-1}) [a]	Initial β-pinene (ppb)	β-pinene reacted (ppb)	$[OH]/10^7$ (cm^{-3})	PM_{max} $(\mu g\ m^{-3})$ [b]
1.9	3.8	3.6	12.5	4.2
1.9	9.2	8.8	11.3	6.5
1.9	9.2	8.9	11.3	6.9
1.9	9.2	8.9	11.3	7.7
1.9	15.9	14.8	6.2	14.4
1.9	24.8	22.0	3.7	23.8
1.9	24.8	22.0	3.7	23.2
1.9	24.8	22.0	3.7	22.0
5.4	3.8	3.6	12.5	4.1
5.4	9.2	9.0	14.5	9.8
5.4	15.9	15.5	15.7	21.3
5.4	24.8	23.9	12.4	39.6

3 [a] J (O^{1}D) was varied by altering the TUV gap
4 [b] Maximum formed particle mass concentration, assuming an SOA density of 1.2 g cm^{-3}. These values have been
5 adjusted for wall losses and losses on particles.
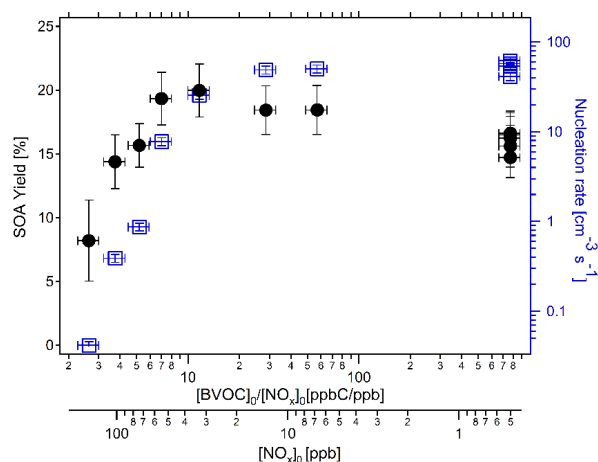
Figure 1. Measured SOA yield from PM_{max} (black circles) and rates of new particle formation (blue squares) for the β-pinene photooxidation as a function of the ratio of the initial hydrocarbon to the initial NO_x concentration and as a function of the initial NO_x concentration. Each point corresponds to one experiment. The errors in nucleation rate and $[NO_x]$ were estimated to be ± 10 %. The error in SOA yield was estimated from error propagation using the sum of the systematic error, correction procedure error and error in BVOC data. Note that the horizontal error bars is associated with the $BVOC/NO_x$ axis.
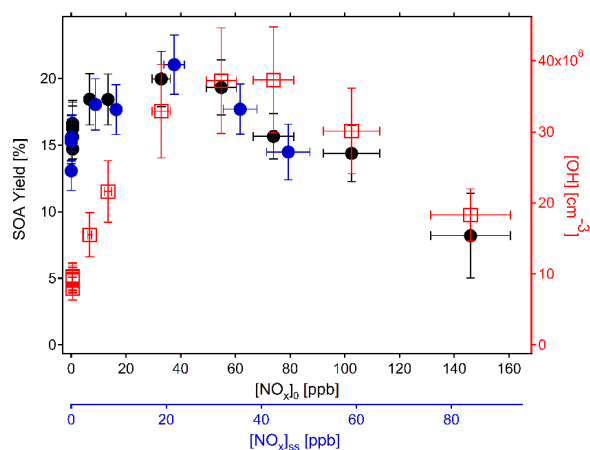
Figure 2. Measured SOA yield from PM_{max} and from steady state PM (black and blue circles respectively) and measured OH concentration (red squares) as a function of initial ($[NO_x]_0$) and steady state ($[NO_x]_{ss}$) NO_x concentrations. The errors in [OH] and $[NO_x]$ were estimated to be ± 20 % and ± 10 % respectively. The error in SOA yield was estimated from error propagation using the sum of the systematic error, correction procedure error and error in BVOC data.
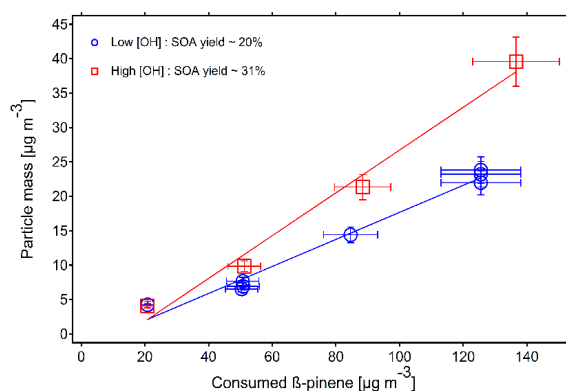
Figure 3. Total aerosol mass concentration as a function of the amount of reacted β-pinene under
low [OH] (blue open circles) and high [OH] (red open squares) conditions. The SOA yield was
estimated from the aerosol mass linear regression slope as a function of consumed β-pinene
which resulted in approximately 20 ± 1 % and 31 ± 3 % for low and high OH conditions
respectively. The error in [consumed β-pinene] was estimated to be ± 10 % and the error in
particle mass was estimated from the sum of the systematic error and the correction procedure
error.
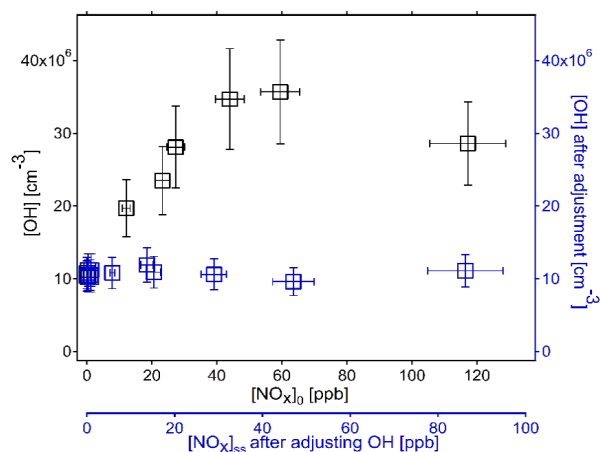
Figure 4. Comparison of [OH] before (black squares) and after (blue squares) adjusting OH
concentration during steady state in NO_x experiments. The errors in [OH] and [NO_x] were
estimated to be ± 20 % and ± 10 % respectively.
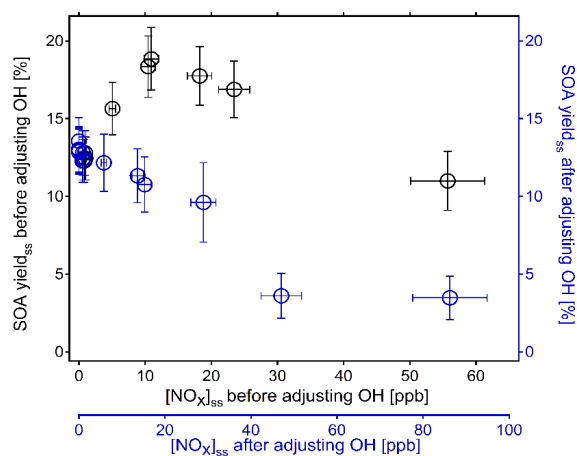
Figure 5. Comparison of SOA yield before (black circles) and after (blue circles) adjusting OH concentration during steady state in NO_x experiments. The error in $[NO_x]$ was estimated to be $\pm$ 10 % and the error in SOA yield was estimated from error propagation using the sum of the systematic error, correction procedure error and error in BVOC data.
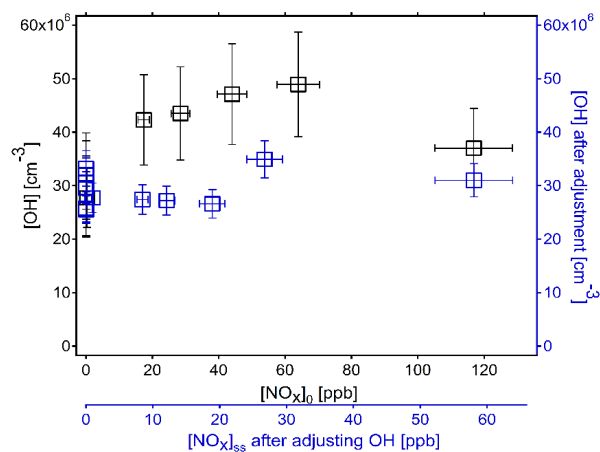
Figure 6. Comparison of [OH] before (black squares) and after (blue squares) adjusting OH concentration during steady state in NO_x experiments performed under lower $[NO]/[NO_2]$ ratio. The errors in [OH] and $[NO_x]$ were estimated to be $\pm$ 20 % and $\pm$ 10 % respectively.
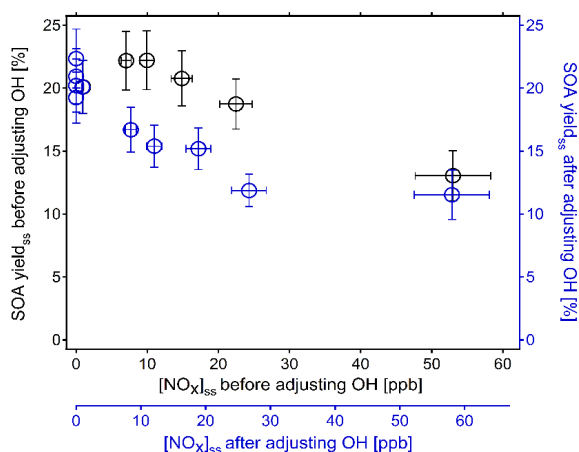
Figure 7. Comparison of SOA yield before (black circles) and after (blue circles) adjusting OH
concentration during steady state in NO_x experiments performed under lower $[NO]/[NO_2]$ ratio.
The error in $[NO_x]$ was estimated to be $\pm$ 10 % and the error in SOA yield was estimated from
error propagation using the sum of the systematic error, correction procedure error and error in
BVOC data.
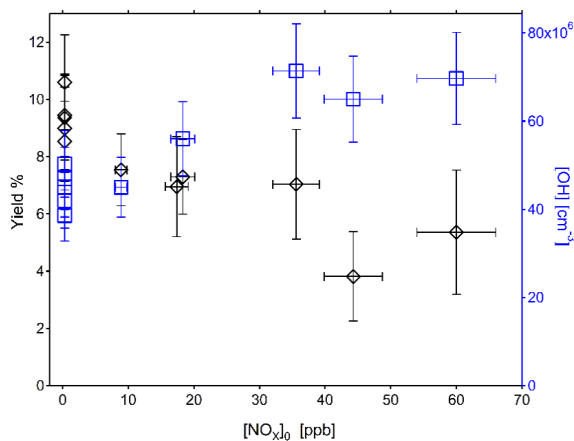
Figure 8. Measured SOA yield (black diamonds) and measured OH concentration (blue squares)
as a function of initial NO_x concentration for α-pinene/NO_x photooxidation experiments. Note
that, due to the lower α-pinene concentrations, the x-axis is not directly comparable to the x-axes
of Fig. 5 and Fig. 7. In sense of BVOC/NO_x ratios, the NO_x range scanned here is ~ 3 times
higher. The errors in [OH] and $[NO_x]$ were estimated to be $\pm$ 15 % and $\pm$ 10 % respectively. The
error in SOA yield was estimated from error propagation using the sum of the systematic error,
correction procedure error and error in BVOC data.
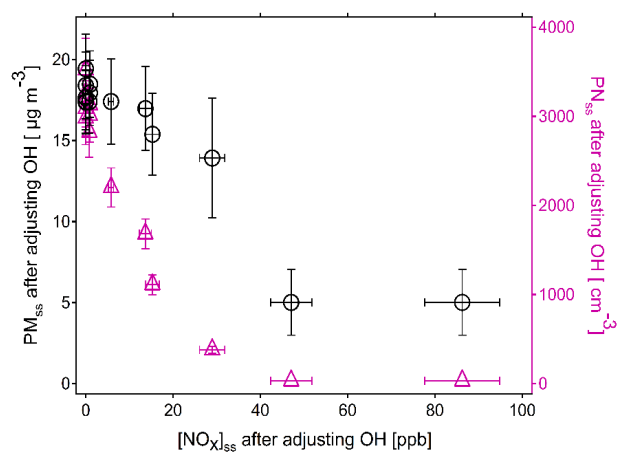
Figure 9. Comparison of measured particle mass and particle number concentration after adjusting [OH] as a function of [NOx] during steady state in the absence of seed aerosol. The error in particle number concentration was estimated to be ± 10 %.
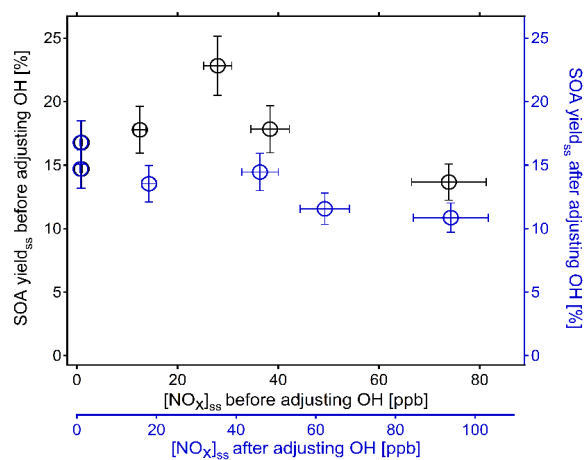
Figure 10. Comparison of SOA yield before (black circles) and after (blue circles) adjusting OH concentration during steady state in NOx experiments performed in the presence of seed aerosol. The error in [NOx] was estimated to be ± 10 % and the error in SOA yield was estimated from error propagation using the sum of the systematic error, correction procedure error and error in BVOC data.